Journal of the European Ceramic Society 20 (2000) 99–106

Electrophoretic deposition of MgO from organic suspensions

B. Ferrari [a,*], R. Moreno [a], P. Sarkar [b,1], P.S. Nicholson [b]

[a] *Instituto de Cerámica y Vidrio. C.I.S.C., Ctra. Valencia km 24,300, 28500 Arganda del Rey, Madrid, Spain*
[b] *Department of Materials Science and Engineering, McMaster University, Hamilton, Ontario, Canada*

Received 28 January 1999; received in revised form 25 April 1999; accepted 11 May 1999

Abstract

MgO is extensively used as a basic refractory material, but in the last decade it has also been considered as a suitable material for technological applications in fields such as catalysis or electronics. Such applications have imposed new requirements regarding the processing techniques. In this way, the electrophoretic deposition (EPD) has been demonstrated to be a useful and simple deposition method among the available coating technologies. A difference with other coating techniques is that the material to be processed by EPD does not require defined properties and hence, there are a wide number of materials that could be coated and deposited by EPD. Major advantages of EPD are versatility, low-cost and reproducibility. The aim of this work was to obtain controlled deposits of MgO onto metallic electrodes by EPD. For this purpose the stability of MgO suspensions in ethanolic media was studied by electrokinetic sonic amplitude (ESA) at different pH conditions. The EPD kinetics was further studied at different electrical conditions. The characteristics of the deposits were studied in relation to the suspension properties and the electrical conditions.

Keywords: MgO; Electrophoretic deposition; Suspensions

1. Introduction

Traditionally MgO has an important role as basic refractory material, but in recent years a wide number of structural and functional applications of MgO based materials have been studied. For example, it has potential applications as a single crystal insulator and tunnel barriers in structural devices[1,2] or as a catalyst, being responsible for the oxidative coupling of methane to produce C2 hydrocarbons.[3,4] Furthermore, MgO is usually considered as a modellic basic oxide often serving as a reference for new applications.

For these reasons, different processing routes for MgO powders[5–12] and their sintering behaviour[12–14] have been studied. In wet processing methods, the strongly basic and the hygroscopic character of MgO make difficult the preparation of either concentrated or diluted suspensions. For concentrated suspensions the rheological measurements are adequate for characterising the slip behaviour. However, the aqueous suspensions of MgO reported for slip casting (>80 wt% solids content) often show a marked thixotropic behaviour, due to the strong surface hydration of MgO powders.[9,10] This limits the obtention of crackless bodies from the mould. On the other hand, when suspensions of low concentration are used, as in EPD processes, the rheological measurements are not useful, and the surface state of the particles requires a deeper study.

MgO is not stable in water, but forms the hydroxide, which easily dissolves. However the precipitation phenomena in Mg^{2+} systems is not only a function of pH, but is very sensitive to atmospheric CO_2, giving place to carbonates. These play a large role at higher pH, as carbonate species become more predominant in the aqueous solutions. The equations governing the solubility of Mg in water are the following:

1. Solids in equilibrium with dissolved species:
   $Mg(OH)_2 \rightarrow Mg^{2+} + 2OH^- \log K_s = 16.84$
   $MgCO_3 \rightarrow Mg^{2+} + (CO_3)^{2-} \log K_s = 7.46$
   $MgCO_3 \cdot 3H_2O \rightarrow Mg^{2+} + (CO_3)^{2-} + 3H_2O \log K_s = -5.19$
   $Mg_4(CO_3)_3(OH)_2 \cdot 3H_2O \rightarrow 4Mg^{2+} + 3(CO_3)^{2-} + 2OH^- \log K_s = -29.5$

2. Dissolved species:
   $Mg^{2+} + H_2O \rightarrow MgOH^+ + H^+ \log K_s = -11.4$
   $MgCO_3(aq) \rightarrow Mg^{2+} + (CO_3)^{2-} \log K_s = -2.88$
   $MgHCO_3^+(aq) \rightarrow Mg^{2+} + HCO_3^- \log K_s = -0.95$

* Corresponding author.
[1] Present address: Alberta Research Council, Advanced Materials Group, Edmonton, AB, Canada T6N 1E4

0955-2219/00/$ - see front matter
PII: S0955-2219(99)00152-1

According to these reactions, when protons are added the concentration of Mg^{2+} ions increases, but in strongly alkaline conditions carbonates precipitate, thus affecting the chemistry of the system. Solubility diagrams can be constructed for Mg diluted in water from these equations taking into account that Mg does not change its redox state.[15]

The high reactivity of MgO in aqueous medium makes it necessary to consider other solvents, such as alcohols or ketones, in which it remains stable. Some authors used organics to slip cast MgO and reached relative densities of 98–99% after sintering at 1450–1600°C.[13,14]

Whichever was the suspension vehicle, stability studies of MgO suspensions, in terms of zeta potential, are not often found in the literature. In 1964, Robinson et al.[16] studied the behaviour of Al_2O_3 and MgO aqueous suspensions and calculated the zeta potential from the Helmholtz–Smoluchowski equation using a streaming potential method.[17] The range of pH studied was between 10 and 14 of a MgO suspension in a 10^{-2}N NaCl. They located the isoelectric point between pH 12 and 13.

Several authors have studied the stability, zeta potential vs pH, of different powders in organic media.[18–20] Brown and Salt[19] studied the electrophoretic deposition of a wide number of materials, measuring the zeta potential of an organic suspension of 50% v/o of MgO by electrophoresis according to a similar equation, where the electrophoretic mobility was obtained with optical microelectrophoresis. They obtained a deposit of MgO on a platinum electrode applying 100 V cm^{-1} from a suspension in ethanol with a zeta potential of 34 mV.

Other kinds of dispersion have been studied by Mizuguchi et al.,[21] who tested the agglomeration and electrosteric dispersion effects of an organic suspension of Al_2O_3 adding nitrocellulose, TMAH and sulphuric acid, as dispersants. After that, they transferred the results to other systems like MgO in ethanol.

Several authors[19,22–24] have studied the electrophoretic deposition behaviour of different systems powder/vehicle, including MgO/ethanol. This system was first reported by Krishna Rao et al.,[11] who made a deep study of the kinetic parameters involved in the electrophoretic deposition of MgO in organics.

The aim of this work is to study the stability of MgO suspensions in ethanol in terms of zeta potential, by the acoustophoresis method, and the viability of EPD in order to obtain homogeneous sinterable deposits. The kinetics of the process has been studied considering the evolution of voltage and slurry conductivity under different experimental conditions.

2. Experimental

A 99.5% purity MgO powder (CERAC, USA) with a density of 2.87 g/cm^3, specific surface area of 85 m^2/g and a mean particle size of 4.9 μm, was used. A fraction of the starting powder was calcined at 1800°C/1 h and subsequently ground by 24 h vibromilling in order to break down the agglomerates originated during calcination. Grinding was made in a plastic jar with Y-TZP balls (5 mm in diameter) using high purity ethanol (0.2 % water). After calcination and grinding, the powder had a density of 3.47 g/cm^3, a specific surface area of 4.5 m^2/g and a mean particle size of 1.6 μm. Surface areas were determined by single point N_2 adsorption, BET (Monosorb, Quantachrome, USA), the particle size distributions with a laser particle size analyser (Mastersizer S, Malvern, UK) and the densities with a He-multipicnometer (Quantachrome, USA). Phase analysis was performed by X-ray diffraction and morphology was observed by scanning electron microscopy.

Titration and zeta potential measurements were performed for suspensions prepared to a solid loading of 1.37% (v/o) by vibromilling for 20 h with Al_2O_3 balls to reduce possible added milling effects. The pH was changed with tetramethylammonium hydroxide (25% methanol, TMAH) and acetic acid (99.7%, HAc) diluted in ethanol to a concentration of 1 M. A wide study of pH stabilisation after the addition of the acid/base, in both kinds of MgO powders suspensions, was made. The slurries were always maintained in a dessicator to avoid exposure to air humidity.

Zeta potential was measured with an Acoustophoresis Equipment MBS 8000 System (MATEC, USA). Electroacoustic method is based on the movement of particles when an alternating voltage is applied to a colloidal dispersion, due to their surface electrical charge. The oscillatory motion of the particles will result in the transfer of momentum to the liquid and the development of an acoustic wave. This effect has been termed Electrokinetic Sonic Amplitude (ESA). ESA is the pressure amplitude generated by the colloid per unit electric field strength and has SI units on Pa $(V\ m)^{-1}$. ESA is exactly analogous to electrophoretic mobility which is represented in terms of velocity normalised by strength of the applied electric field. The mobility by the electroacoustic effect is the dynamic or AC mobility of the particle. The basic equation describing ESA is:[25]

$$\mathrm{ESA}(\omega) = \frac{P}{E} = c\Delta\rho\Phi G_f \mu_d(\omega)$$

where ω is the angular frequency, P is the pressure amplitude of the generated sound wave, E is the amplitude of the applied electric field, c is the velocity of the sound in the suspension, $\Delta\rho$ is the density difference between the particles and the liquid, ϕ is the volume fraction of the particles, G_f is the factor for electrode geometry and μ_d (ω) is the dynamic or high frequency electrophoretic mobility.

For the case of the spherical particles with thin double layers and low zeta potential, the following formula can be applied:[26]

$$\mu_d = \frac{\varepsilon\zeta}{\eta} G(\frac{\omega a^2}{\nu})$$

where a is the particle radius, ε is the dielectric permitivity of the suspension, ν is the kinematic viscosity of the liquid, η is the dynamic viscosity of the liquid and ζ is the zeta potential.

The formula of the dynamic mobility is identical to the well known Smoluchowski equation for the electrophoretic mobility except for the $G(\alpha)$ inertial term. $G(\alpha)$ represents the inertial effect that particles have due to their size, density and mobility, and it is a function of the frequency.

However, the ESA measurements, in opposition to the electrophoretic methods, do not give any information about the sign of the surface charge of the particle. For these reasons, a suspension of particles with known surface charge is used as reference. In this work, a suspension of Al_2O_3 in ethanol with pH 4, which has a positive surface charge,[27] was used. If the signal of ESA angle measured in MgO suspensions is in phase to that of Al_2O_3, then MgO particles at this pH are positive, and negative when the received wave is in opposite phase.

For EPD experiments, suspensions with two different concentrations (1 and 5% v/o) of calcined MgO powder were prepared. EPD was performed using a power supplier which allowed us to work under either constant current intensity or constant voltage conditions. The slips were stirred during the experiment. The stirrer speed was maintained constant in order to assure the same dispersing conditions of suspensions. In the same way, the temperature of the suspensions was maintained constant in order to avoid disturbances in their conductivity evolution.[28]

MgO was deposited onto Ni-coated stainless steel electrodes with an area of 3.6 cm^2 at a constant current density of 0.05 mA cm^{-2} and at a constant voltage of 100 V, varying the deposition time from 30 to 3000 s in both cases. Deposits were weighted immediately after drying. Sintering was performed in air at temperatures of 1600°C and 1650°C for several soaking times. The sintered density was measured by the immersion method.

3. Results and discussion

3.1. MgO characterisation and suspension stability

Phase analysis by XRD of the starting powder reveals the presence of MgO, but the low intensity of the peaks and their width suggested an important hydration degree, which could make difficult slurry preparation and further sintering. This was the reason for calcining the starting powder. The calcined one showed well-defined peaks with better crystallinity.

On the other hand, calcination of a mass of powder promoted the agglomeration and formation of necks, which were broken down by grinding. The particle size distribution of the starting and the calcined and ground powder is shown in Fig. 1. The mean particle size changes from 4.9 μm to 1.6 μm, but in the last case a clear bimodal distribution is observed, probably related to the formation of necks during heat treatment. However, the reduction in surface area is much higher than the reduction in particle size, thus suggesting a higher surface activity in the starting powder.

Fig. 2 shows the morphology of both powders, in which the as-received powder (Fig. 2(a)) shows the agglomerates formed as a consequence of the higher surface activity, while after calcination (Fig. 2(b)) the particle size has decreased.

Both powders were titrated. Several suspensions with a solid content of 1.37% v/o of the as-received MgO were prepared as it was reported above. The pH of the prepared suspension without additives was 12.3. The pH was changed by addition of TMAH and HAc to different values evaluating the time that the suspensions take to reach a stable value of pH. It was observed that the surface state of the particles of MgO suspended in ethanol reached a stable pH when maintained under agitation for 5 min after the acid/base was added, for $pH > 9.5$.

Suspensions of calcined MgO were studied in the same way. The pH measured for these suspensions without

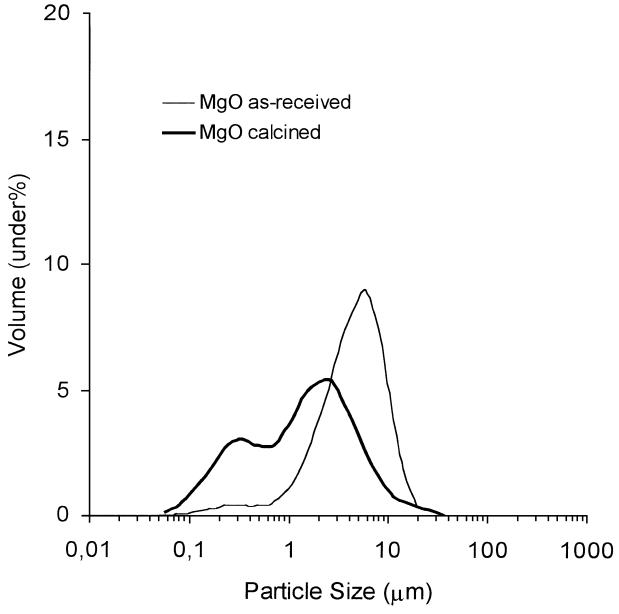

Fig. 1. Particle size distribution of as-received and calcined MgO powders.

additives was 9.1 and the surface state of the particles can be considered stable after 5 min for pH > 7.5.

Fig. 3 shows the titration curves of the as-received and the calcined MgO suspensions, with a solid concentration of 1.37% v/o. In this graphic the volume of TMAH added has been considered negative. Contrarily, the volume of HAc has been considered positive. In the case of calcined MgO, the point of equivalence is sharp and the curve is vertical in this zone, much more than in the case of the as-received powder, in which a gradual variation is observed. This confirms the measurements of the specific surface area, which differ by a factor of 20 between both powders. Accordingly, a much higher quantity of acid is required for the as-received powder compared to the calcined one for a similar change in surface area. As more acid is added the starting powder dissolves more, this consuming protons and, consequently more acid is needed to decrease the pH.

The evolution of zeta potential with pH of both MgO powders is plotted in Fig. 4. In both cases the maximum zeta potential value is obtained for suspensions without acid or base addition. These maxima occur at pH 12.3 and 9.1 for the as-received and the calcined MgO, respectively. Upon addition of acid the concentration of Mg^{2+} increases and then, the concentration of counterions should also increase. As a consequence the zeta potential decreases. When TMAH is added the hydroxyl ions will react with protons in the suspension and pH increases. To counteract the change of pH, protons adsorbed to the powder surface must desorb, so the surface charge and the zeta potential decrease.

It must be noted that the as-received powder shows lower zeta potentials in the whole pH range, which should be related to the higher solubility in good agree-

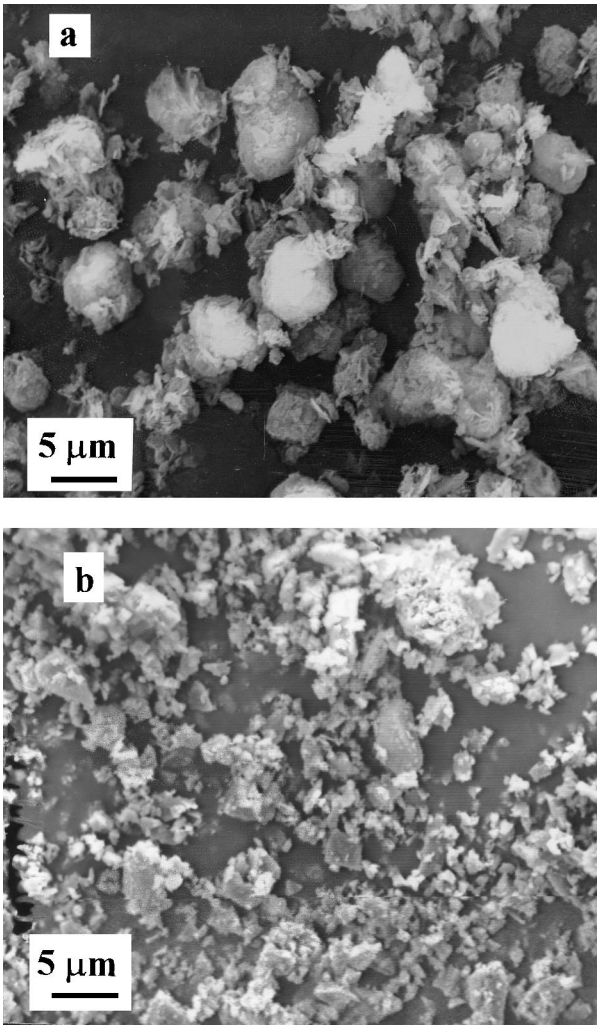

Fig. 2. SEM micrographs of as-received (a) and calcined (b) MgO powders.

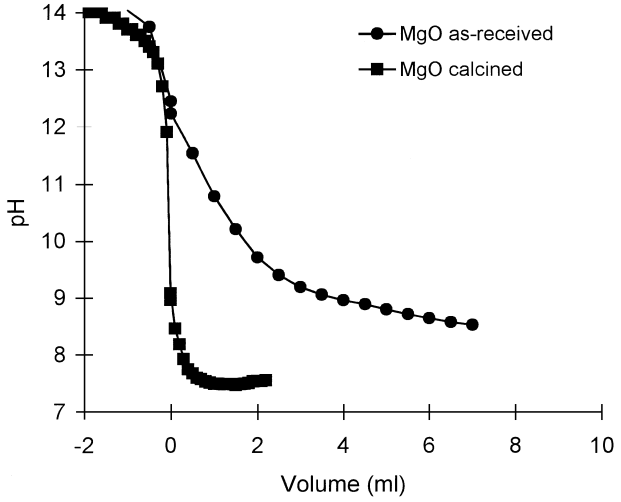

Fig. 3. Titration curves of ethanol suspensions of as-received and calcined MgO powders, adding TMAH and HAc 1 M solutions in ethanol.

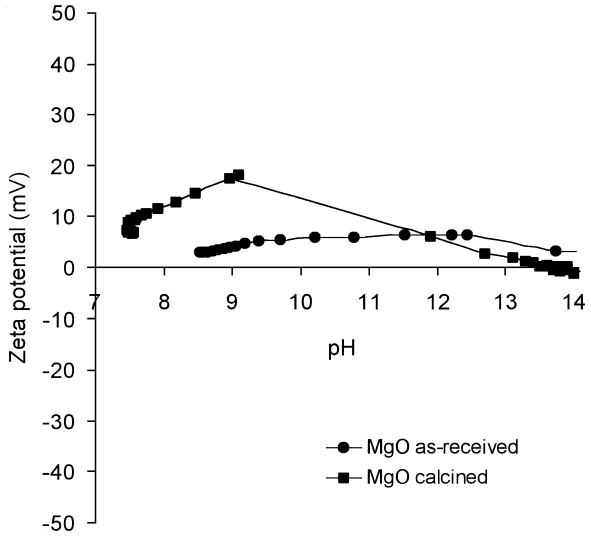

Fig. 4. Zeta potential evolution vs pH of as-received and calcined MgO suspensions in ethanol.

ment with previous data. The isoelectric point of calcined MgO occurs at pH 13.6 ± 0.1, while for the starting MgO no isoelectric point could be detected. The absence of isoelectric point should be again related to the surface state, where the presence of hydrated species promotes an increased isoelectric pH. It has been stated that the isoelectric point of oxides shifts up in about 1.5–2.5 pH units with the hydration degree.[29] In our case, this can be explained because specific adsorption occurs, that is, hydrolizable cations bond to the surface and, consequently, pH_{iep} shifts up. A similar effect has been observed for $BaTiO_3$ powders,[30] where a partial dissolution of the powder leads to readsorption of the Ba^{2+}. From these results it can be assumed that the as-received MgO easily dissolves and the Mg^{2+} ions are readsorbed onto the surface.

All these data indicate that as-received powder will be difficult to process by EPD with the desired constancy of properties, so that calcination becomes necessary to provide the required surface properties for a proper processing. Consequently, EPD studies were performed only for the calcined powder.

3.2. EPD kinetics

In order to assure that the variation of solid concentration during the experiment is negligible, a volume of 250 ml of a 5% v/o suspension of MgO without additives was prepared. The EPD experiment was performed applying a constant current density of 0.05 mA cm^{-2} from 30 to 2000 s (test 1). The results of this study are plotted in Fig. 5 as the relationship between the deposited amount of MgO per unit area and deposition time. As it must be expected in EPD experiments performed at constant current density and constant solid concentration, the amount of deposited material is proportional to the deposition time.[31] The deposition rate for calcined MgO is in a range of 10^{-3} g/cm^2 V^{-1} min^{-1}. This value agrees with other authors, that have worked with MgO in ethanol,[11,12] and lower than the values reported for EPD of MgO suspended in methanol.[23]

EPD tests were also performed using a lower volume of slurry (25 ml), prepared to a lower solid loading (1% v/o) in order to promote a detectable loss-of-powder during deposition. The results of the experiments performed applying a constant current density of 0.05 mA cm^{-2} (test 2) or a constant voltage of 100 V (test 3) from 30 to 3000 s, are plotted in Fig. 6. In this figure the fraction of powder deposited with respect to the total weight of powder tested, is plotted as a function of the deposition time. The kinetics of experiments performed at constant current deviates from the linearity, after a weight fraction of 0.65 of the total starting powder has been consumed during EPD, and the increment of deposited weight related to the increment of deposition time becomes zero. So the deviation is due to the decreased powder concentration in the suspension,[31] and this is the fact stopping the process. For constant voltage conditions the kinetics deviates before (at a weight fraction of 0.5%) because of the decreasing concentration and the differences in the resistivity between the deposit and the suspension.[31] Under constant voltage, the growing deposit is a resistance, thus decreasing the electric field.

Another important observation is that MgO deposits up to 95% of the total weight of the particles in suspension, more than that reported for an Al_2O_3 powder suspended in ethanol.[31]

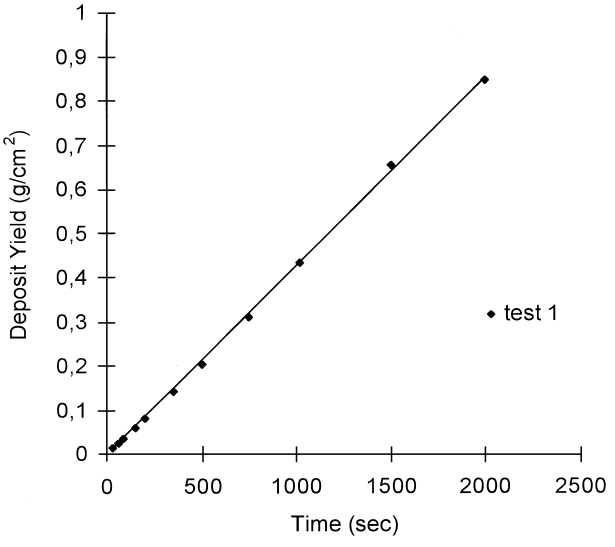

Fig. 5. Deposit yield vs deposition time for the constant current density and constant solid concentrations test (test 1).

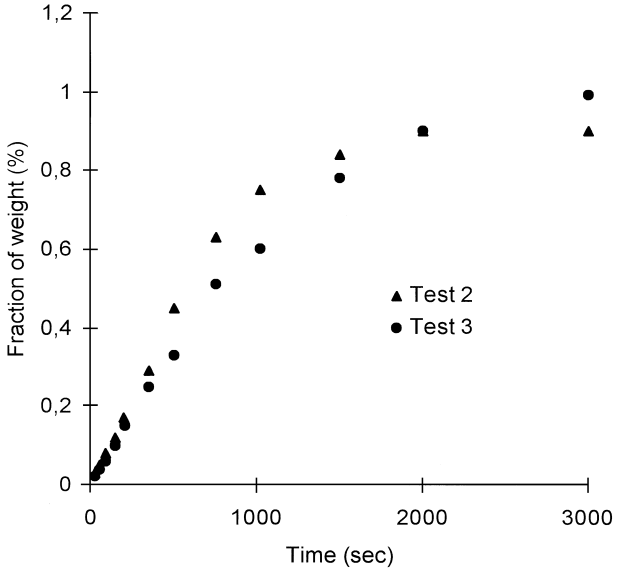

Fig. 6. Fraction of weight vs deposition time for the constant current density test (test 2) and constant voltage test (test 3).

Fig. 7 shows the evolution of voltage measured during the tests performed at constant current density, considering the powder concentration constant (test 1) or time dependent (test 2), and the registered current intensity for EPD tests performed at constant voltage and time dependent concentration (test 3). In test 1, the voltage drop between electrodes remains constant along the experiment. This confirms that the variation of powder concentration in the slurry is negligible for the tested deposition time. Furthermore, the deposit formed in the electrode does not offer a significant resistivity to the applied current intensity. Since the only cathodic reaction in the working electrode is the gas H_2 bubbling, the formed deposit is not being contaminated by electrode corrosion.[28] Then, the conductive character of the deposit should be related to the presence of the specifically adsorbed Mg^{2+} ions on the depositing particles. The total loss of powder in the slurry after the test is only about 13% of the starting suspended mass. The conductivity of the suspension remains constant at around 2 μS cm^{-1} all along the test, due to the low change of solid concentration.

However, in test 2 the voltage increases during the first 500 s, and then starts to decrease, so two different regions in the voltage/time plot can be distinguished. This behaviour can hardly be related to the deposit formation, since a thicker deposit was formed in test 1 for similar conditions and no variation was registered. For test 1 the mass per unit area deposited after 500 s is 0.41 g cm^{-2}, while for test 2 it is 0.12 g cm^{-2}. This suggests that the changes should be directly related to the slurry properties. Among them only two are changing, the conductivity and the concentration, and both are intimately related. Similar effects on slurry conductivity could be detected for tests performed under constant voltage (test 3).

A more precise view of the voltage evolution with deposition time can be obtained when representing the voltage together with the increment of deposit weight for successive EPD tests performed at the conditions of test 2, as it is shown in Fig. 8. In the first region of Fig. 8 the slurry conductivity decreases as powder deposits because of the lowering concentration of charged particles in the slurry. However, there is a point (after 500 s) where the evolution of voltage reverts, that is, suspension conductivity increases. At this point the increment weight falls down also. This is not expected because the constant removal of powder would lead to decreasing conductivities. Assuming again that Mg^{2+} ions are specifically adsorbed, as concluded above, MgO/Mg^{2+} particles and ions are not responsible for the increase of conductivity, since they have been largely consumed (around 45–60% of the starting mass). Therefore, the increase in conductivity must be due to other species in the medium, namely OH- ions, as indicated by the registered increment of pH as H_2 is bubbling in the working electrode. Since charged Mg^{2+} ions would be the first to deposit, when solids are removed the concentration of such ions in the slurry becomes too low to promote any detectable effect. Thus, in the second part of the curves the conductivity increase is only associated to the increase of pH.

To evaluate the influence of processing conditions in the characteristics of the final materials, samples obtained from the three different tests, after deposition times of 750 and 2000 s, were sintered at 1650°C/8 h in air. Table 1 shows the relative sintered density of the deposits measured by the immersion method. It can be

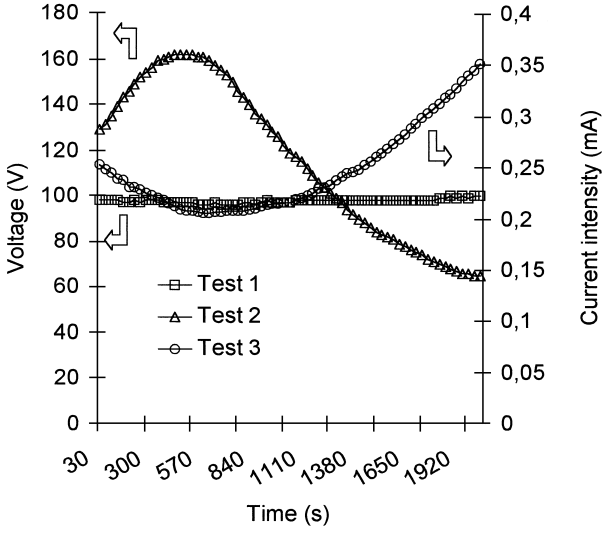

Fig. 7. Voltage evolution vs deposition time for the constant current density tests (tests 1 and 2) and current density evolution vs deposition time for the constant voltage test (test 3).

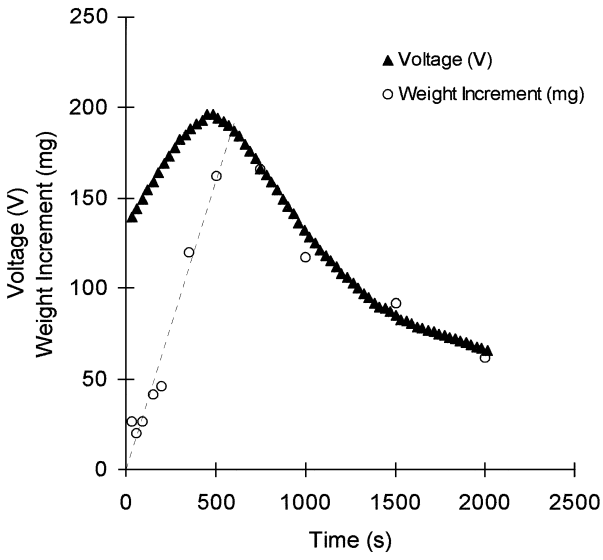

Fig. 8. Evolution of voltage and weight increment vs deposition time when applying a constant current (test 2).

Table 1
Relative density of MgO deposits obtained by EPD under different electric conditions

EPD conditions		Relative density (%)
100 V—1% v/o	750 s	94.7
(test 3)	2000 s	92.5
0.05 mA cm^{-2}—1% v/o	750 s	95.3
(test 2)	2000 s	92.6
0.05 mA cm^{-2}—5% v/o	750 s	95.0
(test 1)	2000 s	97.1

seen that for test 1, a longer deposition time produces a denser deposit, which is consistent with the fact that no variation in the voltage or in the conductivity is registered. A maximum density of 97.1% is reached at these conditions. However, for tests 2 and 3, the maximum density is obtained around the maximum in the voltage versus time curve, thus indicating that the structure of the deposit starts to modify for longer deposition times. On the other hand the maximum density for these tests decreases to around 95%. This confirms the deleterious effect of the reversed behaviour observed in Figs. 7 and 8 originated as a consequence of powder removal in the slurry, so that a simple variation of the solids concentration not only promotes the decrease of the deposition rate, but leads to a deterioration of deposit characteristics, that means, in a loss of the process control.

4. Conclusions

The obtention of uniform and reliable deposits of MgO by electrophoretic deposition in non-aqueous media is described. The starting powders are highly hydrated, thus resulting in both a lower crystallinity and a higher agglomeration. The electrophoretic mobility presents a maximum at pH 12.3, but the isoelectric point cannot be detected, thus confirming the high hydration degree. After calcining, the concentration of surface OH^- groups decreases. As a result, the zeta potential vs pH curve shifts down, so that the maximum value is obtained at pH 9.1 and the isoelectric point is now detected at pH 13.6. Stable suspensions of calcined MgO can be prepared in ethanol at pH 9.

This suspension results in a controlled EPD kinetics, whose deposit yield is proportional to the deposition time up to 3.3 min. When no significant loss of powder occurs, the voltage and the conductivity of the slurry do not change with deposition time. However, when there is an important effect of powder removal, the conductivity starts to decrease, because the concentration of charged particles decreases, but this situation reverts after a certain time, this being hardly related to the particles, but easily associated to the increasing pH. Furthermore, the efficiency of the deposition process under the optimised conditions (related to the suspension parameters and electric experimental conditions) reaches 95% of the total suspended powder.

Dr. B. Ferrari acknowledges C.S.I.C. for the concession of a grant and thanks to Professor Nicholson's research group for their help and friendly reception.

References

1. Smith, D. S., Avedikian, R., Bourg, P., Laval, A., Nussbanum, G. and Borie, J. M., The electrical behaviour of a compressed magnesia powder. *J. Mater. Sci.*, 1994, **29**, 6473–6478.
2. Yadavalli, S., Yang, M. and Flynn, C. P., Low temperature growth of MgO by molecular beam epitaxy. *Phys. Rev.*, 1990, **B41**, 7961.
3. Li, C. and Li, G., FT-IR spectroscopic studies of methane adsorption on magnesium oxide. *J. Phys. Chem.*, 1994, **98**, 1933–1938.
4. Hargreaves, J. S. J., Hutchings, G. J. and Joyner, R. W., *Nature*, 1990, **348**, 428.
5. Huang, R. and Kitai, A. H., The surface morphology of atomic layer deposited magnesia. *J. Mater. Sci. Lett.*, 1993, **12**(18), 1444–1446.
6. Tasai, M. T. and Shih, H. C., Effect of powder processing on the characterization of magnesia derived from alkoxide precursors. I. Preparation and characterization of powders. *J. Mater. Sci.*, 1993, **28**(12), 3391–3397.
7. Tasai, M. T. and Shih, H. C., Effect of powder processing on the characterization of magnesia derived from alkoxide precursors. II. Compaction and sintering behaviour. *J. Mater. Sci.*, 1993, **28**(16), 4530–4535.
8. Viera, J. M. and Brook, R. J., Hot pressing of high-purity magnesium oxide. *J. Am. Ceram. Soc.*, 1984, **67**(7), 450–454.
9. Stoddard, S. D. and Allison, A. G., Casting of magnesium oxide in aqueous slip. *Am. Ceram. Soc. Bull.*, 1958, **37**(9), 409–413.
10. Whiterway, S. G., Coll-Palagos, M. and Masson, C. R., Slip casting of magnesia. *Am. Ceram. Soc. Bull.*, 1961, **40**(7), 432–438.
11. Krishna Rao, D. U. and Subbarao, E. C., Electrophoretic deposition of magnesia. *Am. Ceram. Soc. Bull.*, 1979, **58**(4), 467–469.
12. Lalor, A., Phillips, D. N., Alecu, I. D. and Stead, R. J. Magnesium oxide ceramics produced by slip casting using non-aqueous suspensions. In *Basic-Science Developments in Processing of Advanced Ceramics—Part I*, ed. C. Galassi. Fourth Euro Ceramics, Gruppo Editoriale Faenza Editrice S.p.A., Riccione, Italy, 1995.
13. Wong, B. and Pask, J. S., Experimental analysis of sintering of MgO compacts. *J. Am. Ceram. Soc.*, 1979, **62**(3–4), 141–146.
14. Grupta, T. K., Sintering of MgO: densification and grain growth. *J. Matter. Sci.*, 1971, **6**, 25–32.
15. Smith, R. M. and Martell, A. E. *Critical Stability Constants*, Vol. 4. Plenum, New York, 1976.
16. Robinson, Mc D., Pask, J. K. and Fuerstenau, D. W., Surface charge of alumina and magnesia in aqueous media. *J. Am. Ceram. Soc.*, 1964, **47**(10), 516–520.

17. Fuerstenau, D. W., Measuring zeta potential by streaming potential techniques. *Mining Eng*., 1956, **8**(8), 834–835.
18. Koelmans, H. and Overbeek, J.Th.G., Stability and electrophoretic deposition of suspensions in non-aqueuos media. *Discuss Faraday Soc*., 1954, **18**, 52–63.
19. Brow, D. R. and Salt, F. W., The mechanism of electrophoretic deposition. *J. Appl. Chem*., 1965, **15**, 40–48.
20. Kennedy, H. and Foissy, A., Measurement of mobility and zeta potential of beta-Alumina suspensions in various solvents. *J. Electrochem. Soc*., 1977, **60**, 33–36.
21. Mizuguchi, J., Sumi, K. and Muchi, T., Highly stable nonaqueous suspensions for the electrophoretic deposition of powdered substances. *J. Electrochem. Soc*., 1983, **130**, 1819–1825.
22. Avgustinik, A. I., Vigdergauz, V. S. and Zhuravlev, G. I., Electrophoretic deposition of ceramic masses from suspensions and calculation of deposit yields. *J. Appl. Chem. (URSS)*, 1962, **35**, 2090–2093.
23. Hamaker, H. C., Formation of a deposit by electrophoresis. *Trans. Faraday Soc*., 1940, **36**, 279–287.
24. Hosseinbabaei, F. and Raissidehkordi, B. Impurity dependence of electrophoretic mobility in MgO/Acetone cell. In *Proceedings 9th CIMTEC*. P. Ed. P. Vicenzini, 1999.
25. O'Brien, R. W., Cannon, D. V. and Rowlands, W. N., Electroacoustic determination of particle size and zeta potential. *J. Colloid and Interface Sci*., 1995, **173**, 406–418.
26. MATEC, SA, *Zeta Potential Determination in Concentrated Colloidal Suspension*, *ESA System. Mater. Applied Science*.
27. Nicholson, P. S. and Sarkar, P. The electrophoretic deposition of ceramics. In *Proceedings of the Conference on Ceramic Processing Science and Technology*, Friedrichshafen, Germany, 11–14 September, 1994.
28. Ferrari, B. and Moreno, R., Electrophoretic deposition of aqueous alumina slips. *J. Eur. Ceram. Soc*., 1997, **17**(4), 549–556.
29. Moreno, R., Moya, J. S. and Requena, J., Electroquímica de suspensiones cerámicas. *Bol. Soc. Esp. Ceram. Vidr*., 1987, **26**(6), 355–365.
30. Blanco, M. C., Rand, B. and Riley, F. L., The effect of pH on barium titanate aqueous suspensions. *Key Engineering Materials*, 1997, **132–136**, 305–308.
31. Sarkar, P. and Nicholson, P. S., Electrophoretic deposition (EPD): mechanisms, kinetics, and application to ceramics. *J. Am. Ceram. Soc*., 1996, **79**(8), 1897–2002.